Template Synthesis and Magnetic Characterization of FeNi Nanotubes

**Alena E. Shumskaya[1, *], Egor Yu. Kaniukov[1], Artem. L. Kozlovskiy[2, 3],
Dmitriy I. Shlimas[2, 3], Maxim V. Zdorovets[2, 4], Milana A. Ibragimova[2],
Viacheslav S. Rusakov[5], and Kayrat K. Kadyrzhanov[3]**

Abstract—Iron-nickel nanotubes consisting of 20% Ni and 80% Fe with an aspect ratio of about 100 were synthesized by electrochemical deposition in the pores of polyethylene terephthalate ion-track membranes. The main morphological parameters such as composition, wall thickness and structural characteristics were defined. Macro- and micromagnetic parameters of FeNi nanotubes were determined.

1. INTRODUCTION

Nowadays synthesis of functional nanoscale materials is one of the most attractive areas of research, mainly due to the wide field of potential applications: from electronics, computer technology and communications [1–3] to the biotechnology [4, 5]. Investigation of nanosize structures is an interesting and important task due to possibility to miniaturize devices as well as to understand the unique properties of nanostructures which are different from macrodimension objects [6, 7].

Among the different types of nanostructures the nanotubes (NTs) and nanowires (NWs) can be emphasized due to the large aspect ratio. The simplest and cheapest method of obtaining NTs and NWs is a template synthesis [8–10], which allows the design of metallic [11, 12] or semiconductor [13, 14] NTs and NWs with an aspect ratio of more than 1000 [15]. The method consists in that pores in the templates are filled in with material. Ion-track membranes [16] or matrices of anodized aluminum oxide [17] are usually used as templates. Both types of templates have parallel pores and allow synthesizing NTs and NWs from a diameter of several tens of nanometers.

The use of ion-track membranes provides several advantages when compared with templates based on anodized aluminum oxide, which make them more attractive for practical application. For example, in ion-track membranes it is possible to obtain nanopores with preset shape (cylindrical, conical or double conical), and density in the range from 1 pore per sample to 10^{11} pores/cm^2 [18, 19]. Furthermore, use of the ion-track technology is possible to select the most appropriate material for template according to required physical properties, such as polycarbonate, polyethylene terephthalate, polyimide, glass, and etc. [20–22].

For synthesis of nanostructures with high aspect ratio, there are many methods of pore filling, such as electrochemical deposition [23], an electron-beam lithography [24], chemical vapor deposition [25], pulsed laser deposition [26], and some other methods [27–29]. The most widely used method of metallic nanostructures synthesis is the electrochemical deposition, which allows to efficiently manage the physical and chemical properties of the nanostructures with high degree of process control [8, 17, 23].

Control of the deposition process provides a simple possibility of managing morphological parameters of metallic nanostructures and presetting their functional characteristics. Considering the perspective practical application of magnetic nanoobjects, the important task is to establish the influence of their structure, morphology and crystallinity on the main magnetic parameters and the presence of the magnetic texture.

In this paper, we present a special case of the use of template synthesis method to obtain nanostructures from iron-nickel alloy in the pores of polyethylene terephthalate ion-track membrane by electrochemical deposition, as well as results of detailed study of structural and magnetic parameters of obtained nanostructures.

2. METHODS

Polymer films based on the polyethylene terephthalate of the Hostaphan® type from the "Mitsubishi Polyester Film" (Germany) with thickness of $12\,\mu m$ were used as templates for FeNi nanostructures synthesis. These films had been irradiated with swift heavy ions of krypton with energy of $1.75\,MeV/nucleon$ and fluence of $1.0 \times 10^9\,cm^{-2}$ in the DC-60 accelerator, and latent tracks were etched in the pores in $2.2\,mol/l$ NaOH solution. After etching, pores diameters were $110 \pm 5\,nm$, and their density per unit area was equal to the irradiation fluence. Individual samples with the size of $2.5 \times 2.5\,cm^2$ were cut from these track membranes, which served as a templates for the electrochemical deposition of FeNi NTs. For metal deposition $10\,nm$ gold film electrode (cathode) on PET surface was formed by magnetron sputtering. Templates with sputtered Au thin films were held to the holder tightly to allow access of the electrolyte to the cathode through pores only. Electrochemical synthesis was carried out in the potentiostatic mode at cathode voltages of $1.5\,V$ using the electrolyte of $NiSO_4 \times 7H_2O$ ($110\,g/l$), $FeSO_4 \times 7H_2O$ ($110\,g/l$), $NiCl_2 \times 6H_2O$ ($5\,g/l$), H_3BO_3 ($45\,g/l$), $C_6H_8O_6$ ($1.5\,g/l$) at temperature of $25°C$. The process was controlled chronoamperometrically using the Agilent 34410A multimeter.

Investigations of the structure and morphology of the synthesized FeNi nanostructures were carried out by the scanning electron microscopy (SEM) on the Hitachi TM3030 equipped with the energy-dispersive X-ray analysis (EDX) — the Bruker XFlash MIN SVE with the accelerating voltage of 15 kV. The inner diameters of FeNi NTs were measured by the method of gas permeability using Sartocheck® 3 Plus 16290 at the 0.008–0.020 MPa range of measured pressures.

Precise control of the morphological NTs features was carried out by transmission electron microscopy (TEM) using JEM-100 at an accelerating voltage of $100\,kV$. The crystal structure of the metallic phase was investigated by electron diffraction in the selected area by the JEM-100 TEM and X-ray diffraction (XRD) analysis using the D8 ADVANCE diffractometer with the X-ray tube with Cu anode and graphitic monochromator on the diffracted beam. The XRD patterns were recorded in the range of angles $2\theta \sim 30$–$90°$, with the step $2\theta \sim 0.02°$.

The investigation of macromagnetic properties was carried out using the vibrational magnetometer (the Liquid Helium Free High Field Measurement System (Cryogenic Ltd.)). The measurements were implemented by the induction method, through a determination of the induced electromotive force of the induction in signal coils by a magnetized sample oscillating with a definite frequency at magnetic field $B = \pm 3$ T at 100–300 K temperature.

Mossbauer studies were conducted using spectrometer MS1104Em operating in constant acceleration mode with a triangle-shaped change of doppler velocity of source relatively to the absorber. ^{57}Co cores were used as source in Rh matrix. The Mossbauer spectrometer was calibrated at room temperature using standard a-Fe absorber. The methods for reconstructing distributions of hyperfine parameters of Mossbauer spectra and model fitting using a priori information about object implemented in the program SpectrRelax were used for processing of the Mossbauer spectra.

3. RESULTS AND DISCUSSIONS

In general, the process of electrochemical depositing of metal into the pores of the templates consists of 4 main steps: nucleation, active 1D growth, formation of "caps" on the surface of template and forming a continuous metal thin film on the surface of the template by overlap of the "caps" [30–35]. Chronoamperogramm is shown on Figure 1(a).
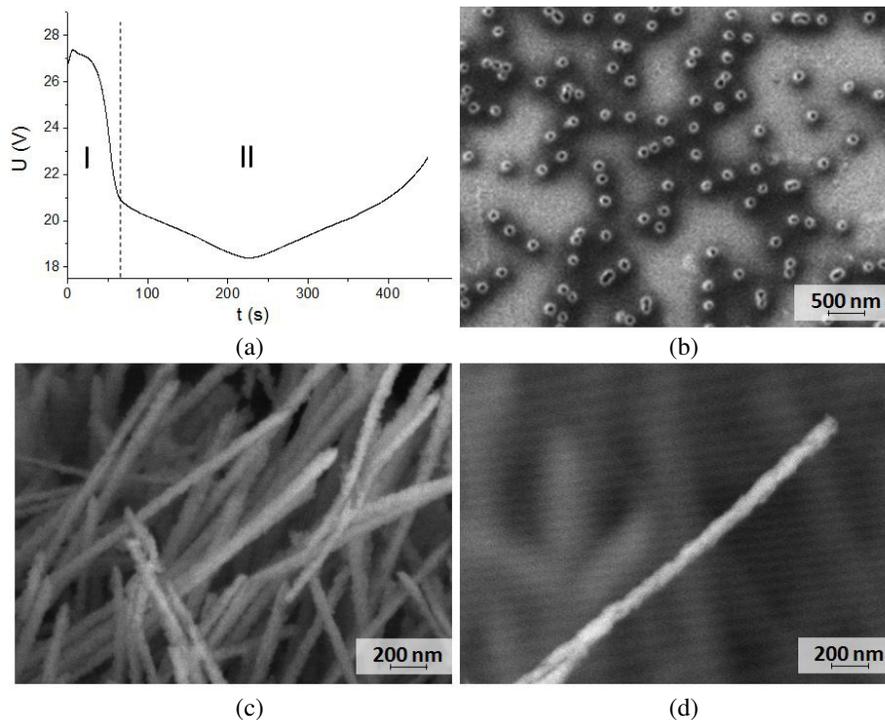
Figure 1. Chronoamperogram of electrochemical deposition process of FeNi nanotubes from electrolyte $NiSO_4 \times 7H_2O$ (110 g/l), $FeSO_4 \times 7H_2O$ (110 g/l), $NiCl_2 \times 6H_2O$ (5 g/l), H_3BO_3(25 g/l), $C_6H_8O_6$ (3 g/l), (a) into pores of PET template. (b)–(c) SEM-images of nanotubes array: (b) in templates; (c) after dissolution of templates; (d) individual nanotube.

Chronoamperogramm consists of two parts, conforming to different deposition stages. The first stage occurs within the first 50 seconds and corresponds to the three-dimensional nucleation on the cathode. The process is characterized by the deposition current of $I = 27$ mA. Further, the current is reducing to 20 mA in the range from 50 to 100 seconds while the second stage of metal deposition in the pores of the templates starts, during which the growth of the precipitate is observed within the pores. This stage is characterized by a slight change of I appearing due to the processes taking place inside pores. SEM image of a metal deposition obtained under selected synthesis conditions, after the removal of the PET template is shown on Figures 1(c), (d).

The SEM image obtained by scanning the sample surface (Figure 1(b)) shows that the nanostructures grow up to the upper border of the template and have the hollow tubes shape. Analysis of the SEM images of structures after removal from PET (Figures 1(c)–(g)) allows determining the length of NTs and their outer diameters. Their length corresponds to the thickness (12 μm) and their diameters — to diameters of template pores (110 nm). Due to the insufficient resolution of SEM and small detentions of FeNi NTs inner NTs diameter d was estimated by gas permeability method. The experimental dependence of internal diameters of FeNi NTs from applied pressure is shown on Figure 2(a), whereby d is ~ 70 nm. The NT wall thickness is ~ 20 nm. Analysis of TEM images (Figure 2(b)) allows evaluating geometric dimensions of NTs, and also indicates the dispersed structure of the walls, which consist of individual crystallites with an average size of ~ 10 nm.

Determination of elemental and phase composition of NTs, as well as their crystalline structure was held by EDA technique and X-ray diffraction. Based on the results of EDA spectra analysis the atomic metal ratio was determined as 20% of Ni and 80% of Fe. The crystal structure of FeNi NTs was assessed on the basis of the electron diffraction patterns analysis in the selected area (inset in Figure 2(b)) and X-ray diffraction spectra (Figure 2(c)).

Electron diffraction pattern allows to make a conclusion that NTs material has a high crystallinity degree and contains separate twinning planes, which arise due to the disorientation of individual
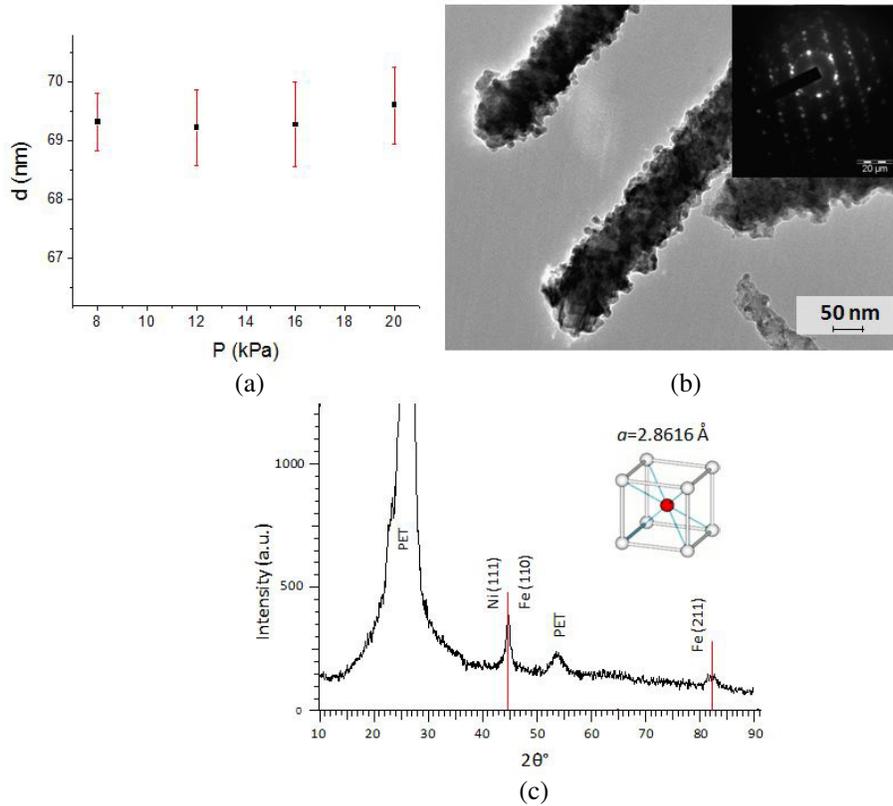
Figure 2. The morphological and structural characterization of FeNi nanotubes: (a) data of gas permeability measurements of the internal diameters pores; (b) TEM-image with a insert of electron diffraction image; (c) diffraction pattern.

crystallites forming NTs wall structure. Reflexes distribution indicates a preferred direction (110), confirmed by the presence of a single peak at $2\theta = 44.752°$ on XRD spectrum. The peak with the angular position of $2\theta = 53$–$54°$ belongs PET pattern [36, 37].

Analysis of the X-ray diffraction data shows *bcc* (body centered cubic) lattice ordering of NTs with lattice parameters $a = 2.8616$Å, compared with the reference value of $a = 2.866$Å. The difference between the reference and obtained value allows one to make an assumption about the lattice strain in NTs due to defects formed during electrodepositing. Also microstrains appear in broadening of symmetrical peak (110) and are caused, on the one hand, by presents of twinning and small average crystallite size, on the other hand. The average crystallite size estimated by the Scherrer equation [38] was set up as 11.56 nm, which corresponds to the value received by TEM.

Measurements of the magnetization dependence on the applied magnetic field $M(H)$ for parallel and perpendicular field orientation relative to the NTs axis were carried out at the temperature of 300 K (Figure 3). Enlarged fragments of the hysteresis loop in the fields up to 0.2 T are on the inset, the main magnetic characteristics of NTs (H_c — coercivity, M_r — residual magnetization, M_s — saturation magnetization) were estimated according to them.

Studying magnetization of FeNi NTs arrays has shown that the behavior of the hysteresis loop is typical for ferromagnetic materials and values of the basic magnetic parameters are closed to values of FeNi NWs [39]. The hysteresis loops obtained for different directions of the magnetic field relative to the main NT axis have different characters, indicating the presence of the magnetic anisotropy in the samples. The values of coercivity for parallel orientation of the field relative to the NTs axis ($H_{c||} = 358$ Oe) are three times higher than the values for the perpendicular direction of the field ($H_{c\perp} = 122$ Oe), and the difference of values of remanent magnetization ($M_{r||} = 60$ emu/g and $M_{r\perp} = 8$ emu/g) is 7.5 times higher. The main determining factors of the magnetic anisotropy presence

in the sample are, mostly, the crystallographic anisotropy and shape anisotropy. The presence of the crystallographic anisotropy is indicated by studies of sample structure — preferred growth direction (110) is coinciding with the direction of the main NTs axis, and the shape anisotropy corresponds to a large aspect ratio (~ 100).

Delicate magnetic parameters of FeNi NTs have been determined by Mössbauer spectroscopy, results are shown in Figure 4.
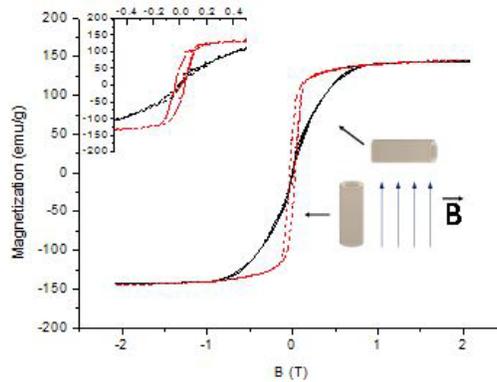

Figure 3. The dependence of magnetization on the applied magnetic field $M(H)$ for NTs in PET template at perpendicular (black solid line) and parallel (red dotted line) direction of the field relative to the NTs axis at $= 300$ K. An enlarged detail of hysteresis loops is shown on insert to figure.
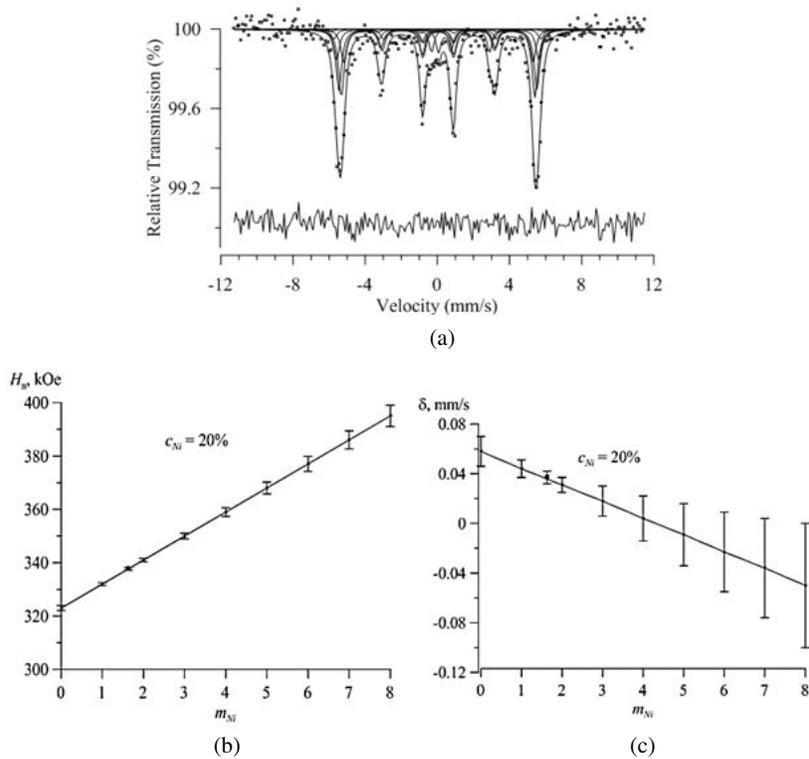

Figure 4. (a) Dependence of Mossbauer spectrum of ^{57}Fe nuclei in FeNi NTs and (b) contributions of hyperfine magnetic field and (c) isomer shift of Mössbauer line on ^{57}Fe nuclei on the number m Ni atoms in the nearest neighborhood of Mössbauer atom.

Mössbauer spectrum of ^{57}Fe nuclei in FeNi NTs is a Zeeman sextet with inhomogeneously broadened lines, which are caused by the existence of non-equivalent positions of Fe atoms in the NTs structure. Spectrum process was carried out in the framework of binomial distribution $P_8(m_{\text{Ni}})$ of Ni atoms on the positions of Fe atoms in α-Fe structure:

$$P_8(m_{\text{Ni}}) = \frac{8!}{m_{\text{Ni}}!(8 - m_{\text{Ni}})!} c^{m_{\text{Ni}}}(1 - c)^{8-m_{\text{Ni}}},$$

c — the Ni atoms concentration, m_{Ni} — number of Ni atoms in the nearest neighborhood of Fe atoms.

It was assumed equidistant variation of hyperfine magnetic field H_n and isomer shift δ of the partial Mössbauer spectrum with increase of the number of Ni atoms in the nearest neighborhood of Fe atoms. The spectrum analysis has showed that values of the hyperfine field H_n increase at the ^{57}Fe nuclei, and the isomer shift δ decreases with the m_{Ni} growth. The displacement of one Fe atom to Ni atom has led the hyperfine magnetic field growth at 7.6 ± 0.8 kOe. Herewith the shift of the Mossbauer line δ has reduced by 0.013 ± 0.007 mm/c. The average value of the hyperfine magnetic field $\bar{H}_n$ is 337.7 ± 0.4 kOe and the isomer shift δ is 0.040 ± 0.006 mm/s at the nuclei of ^{57}Fe. The ratios of the intensities of the second and the fifth to the sixth and the first resonance lines observed Zeeman sextet $\text{I}_{2,5}/\text{I}_{1,6} = 0.38 \pm 0.03$ indicates the existence of magnetic texture with predominant direction along the NTs axis. The average value of the angle between the superfine magnetic field vector and geometric NTs axis is $37.9 \pm 1.1°$.

4. CONCLUSIONS

Iron-nickel nanotubes consisting of 20% Ni and 80% Fe with a length of $12 \, \mu$m, diameter of 110 nm and wall thickness of 20 nm were synthesized by electrochemical deposition in the pores of PET templates. NTs have a polycrystalline structure with an average crystallite size about 12 nm. FeNi NTs have bcc crystal structure with lattice parameter $a = 2.8616$Å. Values of the main magnetic parameters are comparable with the values of the FeNi NWs with corresponding sizes, and NTs have magnetic anisotropy, caused by the presence of crystallographic anisotropy and shape anisotropy. In the NTs there is the oriented along a preferred direction (110) magnetic texture. Magnetic NTs could be used in nano- and microelectronics as elements of flexible electronic circuits and in biomedicine as carriers for drug delivery system and for magnetic separation of biomolecules.

REFERENCES

1. Sander, M. S., M. J. Côté, W. Gu, B. M. Kile, and C. P. Tripp, "Template-assisted fabrication of dense, aligned arrays of titania nanotubes with well-controlled dimensions on substrates," *Adv. Mater.*, Vol. 16, No. 22, 2052–2057, Nov. 2004.

2. Graham, L. M., S. Cho, S. K. Kim, M. Noked, and S. B. Lee, "Role of boric acid in nickel nanotube electrodeposition: A surface-directed growth mechanism," *Chem. Commun.*, Vol. 50, No. 5, 527–529, 2014.

3. Alnassar, M., A. Alfadhel, Y. P. Ivanov, and J. Kosel, "Magnetoelectric polymer nanocomposite for flexible electronics," *J. Appl. Phys.*, Vol. 117, No. 17, 17D711, 2015.

4. Yen, S. K., P. Padmanabhan, and S. T. Selvan, "Multifunctional iron oxide nanoparticles for diagnostics, therapy and macromolecule delivery," *Theranostics*, Vol. 3, No. 12, 986–1003, 2013.

5. Salem, A. K., P. C. Searson, and K. W. Leong, "Multifunctional nanorods for gene delivery," *Nat. Mater.*, Vol. 2, No. 10, 668–671, 2003.

6. Rawtani, D., T. Sajan, A. T. R, and Y. K. Agrawal, "Emerging strategies for synthesis and manipulation of nanowires: A Review," *Rev. Adv. Mater. Sci.*, Vol. 40, No. 2, 177–187, 2015.

7. Guo, P., C. R. Martin, Y. Zhao, J. Ge, and R. N. Zare, "General method for producing organic nanoparticles using nanoporous membranes," *Nano Lett.*, Vol. 10, 2202–2206, 2010.

8. Martin, C. R., "Nanomaterials: A membrane-based synthetic approach," *Science*, Vol. 266, No. 5193, 1961–1966, 1994.

9. Hulteen, J. C. and C. R. Martin, "A general template-based method for the preparation of nanomaterials," *J. Mater. Chem.*, Vol. 7, No. 7, 1075–1087, 1997.

10. Schönenberger, C., "Template synthesis of nanowires in porous polycarbonate membranes: electrochemistry and morphology," *J. Phys. Chem. B*, Vol. 5647, No. 96, 5497–5505, 1997.

11. Ohgai, T., X. Hoffer, A. Fabian, L. Gravier, and J.-P. Ansermet, "Electrochemical synthesis and magnetoresistance properties of Ni, Co and Co/Cu nanowires in a nanoporous anodic oxide layer on metallic aluminium," *Journal of Materials Chemistry*, Vol. 13, No. 10. 2530, 2003.

12. Shao, P., G. Ji, and P. Chen, "Gold nanotube membranes: Preparation, characterization and application for enantioseparation," *J. Memb. Sci.*, Vol. 255, No. 1–2, 1–11, Jun. 2005.

13. Xu, D., Y. Xu, D. Chen, G. Guo, L. Gui, and Y. Tang, "Preparation and characterization of CdS nanowire arrays by dc electrodeposit in porous anodic aluminum oxide templates," *Chem. Phys. Lett.*, Vol. 325, No. 4, 340–344, Jul. 2000.

14. Katwal, G., M. Paulose, I. A. Rusakova, J. E. Martinez, and O. K. Varghese, "Rapid growth of zinc oxide nanotube–nanowire hybrid architectures and their use in breast cancer-related volatile organics detection," *Nano Lett.*, Vol. 16, No. 5, 3014–3021, May 2016.

15. Wang, X. W., Z. H. Yuan, and B. C. Fang, "Template-based synthesis and magnetic properties of Ni nanotube arrays with different diameters," *Mater. Chem. Phys.*, Vol. 125, No. 1–2, 1–4, 2011.

16. Toimil-Molares, M. E., "Characterization and properties of micro- and nanowires of controlled size, composition, and geometry fabricated by electrodeposition and ion-track technology," *Beilstein J. Nanotechnol.*, Vol. 3, No. 1, 860–883, Dec. 2012.

17. Vivas, L. G., Y. P. Ivanov, D. G. Trabada, M. P. Proenca, O. Chubykalo-Fesenko, and M. Vázquez, "Magnetic properties of Co nanopillar arrays prepared from alumina templates," *Nanotechnology*, Vol. 24, No. 10, 105703, 2013.

18. Dallanora, A., T. L. Marcondes, G. G. Bermudez, P. F. P. Fichtner, C. Trautmann, M. Toulemonde, and R. M. Papaléo, "Nanoporous SiO$_2$/Si thin layers produced by ion track etching: Dependence on the ion energy and criterion for etchability," *J. Appl. Phys.*, Vol. 104, No. 2, 24307–1–24307–8, 2008.

19. Fink, D., *Fundamentals of Ion-Irradiated Polymers: Fundamentals and Applications. V. 1*, Springer, Berlin-Heidelberg, 2004.

20. Shen, C., X. Wang, W. Zhang, and F. Kang, "Direct prototyping of patterned nanoporous carbon: A route from materials to on-chip devices," *Sci. Rep.*, Vol. 3, 2294, 2013.

21. Kaniukov, E. Y., J. Ustarroz, D. V Yakimchuk, M. Petrova, H. Terryn, V. Sivakov, and A. V Petrov, "Tunable nanoporous silicon oxide templates by swift heavy ion tracks technology," *Nanotechnology*, Vol. 27, No. 11, 115305, Mar. 2016.

22. Fink, D., A. V. Petrov, K. Hoppe, W. R. Fahrner, R. M. Papaleo, A. S. Berdinsky, A. Chandra, A. Chemseddine, A. Zrineh, A. Biswas, F. Faupel, and L. T. Chadderton, "Etched ion tracks in silicon oxide and silicon oxynitride as charge injection or extraction channels for novel electronic structures," *Nucl. Instruments Methods Phys. Res. Sect. B Beam Interact. with Mater. Atoms*, Vol. 218, No. 1–4, 355–361, 2004.

23. V. Haehnel, S. Fähler, P. Schaaf, M. Miglierini, C. Mickel, L. Schultz, and H. Schlörb, "Towards smooth and pure iron nanowires grown by electrodeposition in self-organized alumina membranes," *Acta Mater.*, Vol. 58, No. 7, 2330–2337, 2010.

24. Martín, J. I., M. Vélez, R. Morales, J. M. Alameda, J. V. Anguita, F. Briones, and J. L. Vicent, "Fabrication and magnetic properties of arrays of amorphous and polycrystalline ferromagnetic nanowires obtained by electron beam lithography," *J. Magn. Magn. Mater.*, Vol. 249, Nos. 1–2, 156–162, Aug. 2002.

25. Barth, S., S. Estrade, F. Hernandez-Ramirez, F. Peiro, J. Arbiol, A. Romano-Rodriguez, J. R. Morante, and S. Mathur, "Studies on surface facets and chemical composition of vapor grown one-dimensional magnetite nanostructures," *Cryst. Growth Des.*, Vol. 9, No. 2, 1077–1081, Feb. 2009.

26. Morber, J. R., Y. Ding, M. S. Haluska, Y. Li, J. P. Liu, Z. L. Wang, and R. L. Snyder, "PLD-assisted VLS growth of aligned ferrite nanorods, nanowires, and nanobelts-synthesis, and properties," *J.*

Phys. Chem. B, Vol. 110, No. 43, 21672–21679, 2006.

27. Liu, Z., Q. Zhang, G. Shi, Y. Li, and H. Wang, "Solvothermal synthesis and magneto-optical properties of Zn1-xNixO hierarchical microspheres," *J. Magn. Magn. Mater.*, Vol. 323, No. 7, 1022–1026, Apr. 2011.

28. Hua, Z., S. Yang, H. Huang, L. Lv, M. Lu, B. Gu, and Y. Du, "Metal nanotubes prepared by a sol-gel method followed by a hydrogen reduction procedure," *Nanotechnology*, Vol. 17, No. 20, 5106–5110, 2006.

29. Zhou, D., T. Wang, M. G. Zhu, Z. H. Guo, W. Li, and F. S. Li, "Magnetic interaction in FeCo alloy nanotube array," *J. Magn.*, Vol. 16, No. 4, 413–416, 2011.

30. Yoo, B., F. Xiao, K. N. Bozhilov, J. Herman, M. A. Ryan, and N. V. Myung, "Electrodeposition of thermoelectric superlattice nanowires," *Adv. Mater.*, Vol. 19, No. 2, 296–299, 2007.

31. Motoyama, M., Y. Fukunaka, T. Sakka, and Y. H. Ogata, "Initial stages of electrodeposition of metal nanowires in nanoporous templates," *Electrochim. Acta*, Vol. 53, No. 1, 205–212, Nov. 2007.

32. Narayanan, T. N., M. M. Shaijumon, L. Ci, P. M. Ajayan, and M. R. Anantharaman, "On the growth mechanism of nickel and cobalt nanowires and comparison of their magnetic properties," *Nano Res.*, Vol. 1, No. 6, 465–473, Dec. 2008.

33. Proenca, M. P., C. T. Sousa, J. Ventura, M. Vazquez, and J. P. Araujo, "Distinguishing nanowire and nanotube formation by the deposition current transients," *Nanoscale Res. Lett.*, Vol. 7, No. 1, 280, 2012.

34. Han, X.-F., S. Shamaila, R. Sharif, J.-Y. Chen, H.-R. Liu, and D.-P. Liu, "Structural and magnetic properties of various ferromagnetic nanotubes," *Adv. Mater.*, Vol. 21, No. 45, 4619–4624, Dec. 2009.

35. Narayanan, T. N., M. M. Shaijumon, P. M. Ajayan, and M. R. Anantharaman, "Synthesis of high coercivity cobalt nanotubes with acetate precursors and elucidation of the mechanism of growth," *J. Phys. Chem. C*, Vol. 112, No. 37, 14281–14285, Sep. 2008.

36. Guillén, C. and J. Herrero, "Comparison study of ITO thin films deposited by sputtering at room temperature onto polymer and glass substrates," *Thin Solid Films*, Vol. 480–481, 129–132, Jun. 2005.

37. Faraj, M. G. and K. Ibrahim, "Optical and structural properties of thermally evaporated zinc oxide thin films on polyethylene terephthalate substrates," *Int. J. Polym. Sci.*, Vol. 2011, 1–4, 2011.

38. Langford, J. I. and A. J. C. Wilson, "Scherrer after sixty years: A survey and some new results in the determination of crystallite size," *J. Appl. Crystallogr.*, Vol. 11, No. 2, 102–113, Apr. 1978.

39. Han, G. C., B. Y. Zong, P. Luo, and Y. H. Wu, "Angular dependence of the coercivity and remanence of ferromagnetic nanowire arrays," *J. Appl. Phys.*, Vol. 93, No. 11, 9202–9207, 2003.